1. AGENCY USE ONLY (Leave blank)	2. REPORT DATE	3. REPORT TYPE AND DATES COVERED
	8/11/93	Final Technical Report 3/15/91 – 3/15/93

4. TITLE AND SUBTITLE

Heat Transfer and Flow Structure in End-Wall Boundary Layers

5. FUNDING NUMBERS

AFOSR-91-0218

2307/DS

6. AUTHOR(S)

C. R. Smith and J. D. A. Walker

7. PERFORMING ORGANIZATION NAME(S) AND ADDRESS(ES)

Lehigh University
Department of Mechanical Engineering
354 Packard Lab #19
Bethlehem, Pennsylvania 18015

AFOSR-TR- 5

8. PERFORMING ORGANIZATION REPORT NUMBER

533024

9. SPONSORING/MONITORING AGENCY NAME(S) AND ADDRESS(ES)

N A

AFOSR
Bolling Air Force Base
Washington, D. C. 20332

10. SPONSORING/MONITORING AGENCY REPORT NUMBER

AFOSR—
91-0218

11. SUPPLEMENTARY NOTES

12a. DISTRIBUTION/AVAILABILITY STATEMENT

12b. DISTRIBUTION CODE

DISTRIBUTION STATEMENT A
Approved for public release; Distribution Unlimited

13. ABSTRACT *(Maximum 200 words)*

Research progress is described for a combined analytical/experimental program examining the flow structure and resultant surface heat transfer in end-wall boundary layers (e.g. wing-body type junctures). Emphasis is placed on flow structure development and correlation of vortex-induced surface interactions with transient, local surface heat transfer. Analytically, numerical studies using an impulsively-started approach flow have documented the flow development and surface heat transfer on the symmetry plane for several end-wall flows; highly unsteady vortex formation and ejection are observed, with concomitant sharp, transient variations in surface heat transfer. Analysis of the complete three-dimensional behavior indicates the presence of strong interactions between the end-wall (surface) and the side-wall (bluff-body) boundary layers. Experimentally, a constant heat flux test system has been developed and instrumented for surface temperature detection using temperature-sensitive liquid crystals and color computer-image analysis; tests indicate dramatic effects of transient end-wall vortices on surface heat transfer, confirming the analytical results. A systematic visualization study indicates a very strong influence of the junction-induced pressure gradient on the approach boundary layer in promoting the unsteady vortex formation processes in the end-wall region.

14. SUBJECT TERMS	15. NUMBER OF PAGES
Three-dimensional, vortex motion, heat transfer, end-wall flows, turbulent boundary layers, fluid mechanics	27
	16. PRICE CODE

17. SECURITY CLASSIFICATION OF REPORT	18. SECURITY CLASSIFICATION OF THIS PAGE	19. SECURITY CLASSIFICATION OF ABSTRACT	20. LIMITATION OF ABSTRACT
Unclassified	Unclassified	Unclassified	

1. SUMMARY

Research progress is described for a combined analytical/experimental program to elucidate the flow structure and resultant surface heat transfer in end-wall boundary layers (e.g. wing-body type junctures). Emphasis is placed on flow structure development and correlation of vortex-induced surface interactions with transient, local surface heat transfer. Numerical studies using an impulsively-started approach flow have documented the flow development and surface heat transfer on the symmetry plane for several end-wall types of flows; highly unsteady vortex formation and ejection are observed, with concomitant sharp, transient variations in surface heat transfer. Analysis of the complete three-dimensional behavior indicates the presence of strong interactions between the end-wall (surface) and the side-wall (bluff-body) boundary layers. Experimentally, a constant heat flux test system has been developed and instrumented for surface temperature detection using temperature-sensitive liquid crystals and color computer-image analysis; tests indicate dramatic effects of transient end-wall vortices on surface heat transfer, confirming the analytical results. A systematic visualization study indicates a very strong influence of the junction-induced pressure gradient on the approach boundary layer in promoting the unsteady vortex formation processes in the end-wall region.

2. OBJECTIVES

The cumulative research effort constitutes a collaborative and interactive two-year effort involving Professors C. R. Smith and J. D. A. Walker and three graduate research assistants in the Department of Mechanical Engineering and Mechanics at Lehigh University. A summary of the research objectives are:

1. To design and develop an experimental test section and evaluation system for examination of the time-dependent flow structure and surface heat transfer in the end-wall region of a bluff body, including a liquid crystal temperature detection surface and color digitizer/image analysis system for evaluation of liquid crystal images.

2. To experimentally examine the transient surface heat transfer induced by transient end-wall vortices over a broad range of Reynolds numbers, correlating surface temperature patterns and behavior with the induced eruptive behavior of the vortices using dual-view examination of the liquid crystal heat transfer surface and hydrogen bubble visualization; to establish the relationship between induced eruptive behavior and locally amplified surface heat transfer.

3. To compute the unsteady viscous flow that develops in the end-wall region for the flow past a cylinder mounted on a flat surface, in order to establish the flow physics of the end-wall region and the influence on surface heat transfer.

4. To compute the surface flow and heat transfer response and eruptive activity due to convected three-dimensional disturbances typical of that induced near the surface by both symmetric and asymmetric hairpin-like vortices; a range of spanwise Reynolds numbers will be considered in order to establish asymptotic trends over a range of Reynolds numbers.

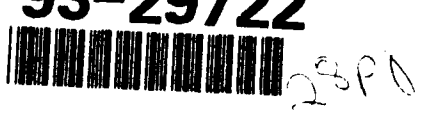

5. To experimentally examine the transient heat transfer due to passage of both controlled hairpin vortices and symmetrically generated turbulent spots, employing the results of both the controlled vortex experiments and the computations to guide the study.

6. To employ the experimental test system to examine the comparative and contrasting changes in transient surface heat transfer with an impinging low-speed, low Reynolds number, turbulent boundary layer.

7. To synthesize the physics of vortex-induced surface heat transfer from the combined computational/experimental results allowing development of a physical model of the key processes impacting convective heat transfer in turbulent boundary layers and other vortex-dominated flows.

3. DESCRIPTION OF RESEARCH

3.1 Introduction

Three-dimensional juncture flows are common in a variety of applications including wing/body junctions and the base of the turbine blade at the hub. It is generally supposed in the literature that some type of steady horseshoe-vortex configurations exist near such junctures and the limited number of attempts that have been made to compute and/or explain the physics of such flows have usually been based on this premise. However, recent experiments indicate that at high Reynolds, the flow near such a juncture is far from being steady and exhibits a rich variety of complex unsteady separation effects. The simplest type of juncture flow, which is under consideration in this study, is depicted schematically in Figure 1. Here an oncoming boundary layer on a flat surface encounters a circular cylinder mounted normal to an end wall.

The geometry shown in Figure 1 may be regarded as a model problem which captures the essential elements of more general juncture flows. In fact, turbine blade shapes and rectangular blocks have also been studied and found to give essentially the same type of flow field. Hence this type of important geometry yields an essentially generic flow behavior. Experiments carried out by Greco and Smith (1991) show that in addition to the expected separation and vortex shedding from the upright cylinder, three-dimensional separation occurs in the end-wall boundary layer. This separation takes the form of evolving necklace vortices that originate on the upstream symmetry plane of the cylinder and apparently spread rapidly outboard. The vortices are expected to form due to the adverse pressure gradient immediately upstream of the cylinder. The mode in which they rapidly spread around the cylinder downstream is not well understood. At a certain stage, the vortices on the symmetry plane become interactive and induce an eruptive flow from the symmetry plane. This appears to cause the ejection of vortices from the end-wall layer wherein they are convected toward the cylinder and then appear to dissipate. In addition to this effect, the arms of the vortices sweep around towards the cylinder and ultimately provoke boundary layer eruptions of the end-wall flow, thus giving rise to the production of hairpin vortices. This is shown schematically in Figure 1b [see also Smith et al., 1991].

This flow therefore contains a rich variety of unsteady three-dimensional separation phenomena, the physics of which are poorly understood. Recently, Visbal (1991) has carried out a numerical simulation of this flow [see also Hung et al. 1991), which gives results that are apparently consistent with many of the gross experimental

observations of Greco and Smith (1991). These calculations have been carried out at relatively low Reynolds numbers and the results have been somewhat controversial. On average, each simulation required over one hundred hours of CRAY time and due to computer memory and CPU time limitations, a relatively course mesh had to be utilized in some portions of the flow field. It is therefore very difficult to reach the high Reynolds number range with a direct numerical simulation. For this reason, the present analytical work is concerned with the high Reynolds number limit and trying to isolate how the necklace vortices form and their subsequent dynamical evolution.

In this study, a particular aspect of importance is the influence of heat transfer near the surface and how this is affected by the formation and evolution of the vortices above. It was found that the processes of heat transfer in the end-wall boundary layer are dominated by the dynamics of the vortex motion. A major thrust of both the experimental and analytical work was to establish the physics of the process of heat transfer due to end-wall vortex dynamics.

3.2 Analytical Resultss

At high Reynolds numbers in the end-wall flows, it is observed that there is a periodic vortex formation eruption and then a new vortex formation. Consequently, to understand the processes of formation, it is sufficient to look at the situation of impulsively-started motion past an obstacle and to track the boundary layer events that develop forward in time. With reference to Figure 1a, it may be inferred that there is a complex boundary layer structure that forms in this geometry. There is an end-wall boundary layer along the flat surface, sidewall boundary layers along the cylinder, and a region in the corner where the two boundary layers merge. The flow evolution, particularly in the end-wall boundary layer, is completely three-dimensional. However, there is also an upstream and downstream symmetry plane, as indicated schematically in Figure 1b, where the flow in the end-wall layer develops independent of the outboard flow. Of particular interest is the upstream symmetry plane where it is expected that vortices form under the action of the adverse pressure gradient due to the cylinder. Because of the complexity of the problem, it is necessary to develop a systematic approach for analyzing each of these regions. In the research, the following tasks were accomplished:

3.2.1 Numerical solutions have been obtained for the developing flow on the symmetry plane upstream of the cylinder in the end-wall boundary layer. These calculations show the formation of the three-dimensional vortex structure which forms on the upstream symmetry plane. The streamline development following an impulsive start is shown in Figure 2. It may be seen that the flow structure in relatively complicated. There is a saddle point located at a distance off the wall and a spiral vortex above this. The flow enters this spiral vortex and then moves off the symmetry plane, presumably initiating formation of a necklace vortex. Numerical solutions have also been carried out along the downstream symmetry plane and these show basically a featureless accelerated flow. The interesting aspects are always associated with the adverse pressure gradient on the upstream symmetry plane. Currently, calculations have been carried out using a Eulerian formulation with upwind-downwind differencing for the convective terms. A complex sequence of events (shown in Figure 2) is observed to ensue. Beyond the stage shown in Figure 2(c), the vortex continues to move in the upstream direction and then appears to undergo a sharp compression during which fluid is violently ejected upward out of the boundary layer. This is believed to be the onset of a three-dimensional eruption which is the genesis of

the necklace vortices observed in the experiments near the cylinder. The numerical integrations become progressively less accurate as the flow focuses towards an eruption.

3.2.2 The apparent focussing of the boundary-layer flow into a narrow eruptive spike eventually leads to the failure of the Eulerian algorithm and points to the necessity of developing an alternative formulation. A three-dimensional Lagrangian algorithm was developed to compute the evolution of the motion on the symmetry plane. These integrations are among the first performed in a plane of symmetry Lagrangian formulation (are also Cowley et al., 1991) and show the evolution of a separation singularity at finite time; the streamlines at the singular time are shown in Figure 2(d) where a sharp compression of the spiral vortex may be noted. The sharpness of the eruptive event is also illustrated in Figure 3 where the temporal development of the streamwise and cross-stream displacement thickness show the evolution of sharp spikes. The expected behavior at separation is that a sharply focussed vortex sheet will emerge from the endwall boundary layer and subsequently roll over in a strong viscous-inviscid interaction leading to vortex evolution and then release toward the obstacle.

3.2.3 The influence of the vortex motion on the heat transfer near the symmetry plane has been calculated numerically for the isothermal surface. The calculated results for heat transfer with an isothermal surface have shown that very sharp variations occur in the surface heat transfer in the vicinity of the vortex, and these are particularly accentuated as the boundary layer flow goes into an eruptive mode. Computed results for the surface heat flux are shown in Figure 4(a) and show relatively high heat transfer rates at the cylinder itself (near the stagnation point), as well as a moving zone which progresses upstream and involves an increasingly-focussed region of relatively low heat transfer. The reason for this may be seen in Figure 4(b) where the contours of constant temperature are shown at the instant of separation; it may be seen that the temperature contours are pulled away from the wall near the streamwise station corresponding to separation, as a consequence of the strong upwelling, giving rise to considerably reduced levels of local heat transfer. The results suggest that the processes of heat transfer in the end-wall boundary layer upstream of the obstacle are dominated by the dynamics of the vortex motion. This sharp local change in surface heat flux should give rise to material problems in the end-wall region upstream of the obstacle which is therefore a zone of high thermal stress. The results obtained for heat transfer here are similar to those obtained a number of years ago at UTRC [see Haidari and Smith, 1984]. At the trailing edge of a turbine blade, very sharp changes in the local heat transfer rates were also observed and were believed to be associated with the separation and vortex shedding that took place there.

3.2.4 Because of some of the problems encountered in the full three-dimensional case, a subproblem was considered, wherein a boundary layer encounters a two-dimensional obstacle consisting of a semi-circular hump along a flat wall. Numerical solutions for this case corresponding to both the flow and temperature fields, are calculated. They show that again a separation occurs upstream of the obstacle, which then focuses towards a sharp eruption. Again, the surface heat transfer rates appear to be dominated by the action of the flowfield above and evolve toward a sharply spiked profile as the eruptive event starts to occur. Solutions have been carried out here for both the Eulerian and Lagrangian

system. These calculations were done as an aid toward understanding how to calculate the more complex three-dimensional boundary layer. Calculated streamlines at separation are shown in Figure 5 with temporal development of displacement thickness and wall heat flux shown in Figures 6.

3.2.5 Analysis of the complete three-dimensional end-wall boundary layer and the heat transfer processes taking place is still in progress. In principle, solutions on the two symmetry planes form boundary conditions to allow analysis of the end-wall layer. However, it was determined that the situation is somewhat more complex than this. Evidently, communication is set up between the end-wall boundary layer and the sidewall layer, with the motion becoming interactive at a fairly early stage. In order to isolate the nature of this interaction, an analytic solution was calculated for the initial motion immediately after the impulsive start. The objective of these studies is to understand how the interaction between the two boundary layers takes place and in particular how the end-wall boundary layer behaves near the surface. This work is still currently in progress.

3.3 Experimental Progress

3.3.1 Test Section Development

During the initial year of the grant, the bulk of the experimental effort was devoted to development of the heat transfer test section and instrument acquisition and implementation. Because of the complexity of the measurement and visualization process, a great deal of care had to be taken in the design of the system to assure that the system would be sufficiently responsive for examination of the temporal heat transfer changes anticipated for vortex interactions.

Since the intent of the research is to establish local heat transfer changes based on spatial-temporal variations in surface temperature patterns using thermochromic liquid crystals, this required that the test surface be a constant heat flux surface. After detailed consideration of several options, a test section employing a 40 μm thick stainless steel foil, stretched very tightly, and glued on a 35 cm x 43 cm insulated back was designed and fabricated (see Figure 7). Originally, the foil was stretched over a plastic frame which was sealed on the opposing side by a glass plate, which isolated the interior surface of the foil sheet. However, this arrangement was cumbersome to view and illuminate through the bottom of the water channel, and placing any object on the stretched surface caused a deflection on the surface, which was problematic in maintaining a stable flow. The acquisiton of encapsulated liquid crystals made the use of liquid crystals on the upper, water-contact surface feasible; thus, the final test plate utilized thermochromic liquid crystal paint with a 5° C range applied to the exterior surface of the foil. The liquid crystal paint is mixed with a sealer which makes it function effectively under water for a period of up to two hours; after that period, the paint does absorb water, and must be removed (using a thinner) and the surface recoated. Viewing and illumination of the liquid crystal surface is done through the upper surface of the water channel; normally, two quartz studio lights of 1050 watts each were used for illumination.

To provide a uniformly stretched foil sheet, a stretching frame was designed and constructed, as shown in Figure 8, which can stretch the foil uniformly prior to gluing to the insulated test surface. Electrical contact with the foil is accomplished through two copper bus bars, which are clamped to extensions of the stainless steel foil, providing a uniform conduction path through the foil. The power supply for heating the

foil is designed and fabricated from a welding variac and two step-down transformers; connection to the test surface is done with heavy gage welding cable and connectors. The power supply provides current flow of up to 500 amps to the test surface at an adjusted voltage differential of 5 volts, allowing generation of galvanic heating from 0 to 2500 watts. The use of a low voltage-high current supply eliminates the risk of electrical shock for operation of the test surface in water.

Operation of the test surface in the water channel showed it to be extremely safe and very effective at controlling surface heat transfer over a broad range of power inputs. Calibration data taken (using an image analysis system described below) with a laminar flow suggest temperature uniformity over the test surface of approximately 4% at worst. Additionally, calibration of the liquid crystals with point thermocouple measurements indicate that the correlation of color hue with temperature (as expected) is nonlinear, but with a repeatability of $\pm 3\%$. Further tests of the surface, although difficult to carry out, indicate a frequency response of the test surface of between 8 and 10 Hz; this is consistent with predictions of a lumped parameter model of the test surface, and is a quite acceptable response for the temporal variations encounterd for the low-speed vortex flows of the present study. The biggest factor in the frequency response is the thickness of the liquid crystal coating, which we have been attempting to minimize as we develop expertise in painting of the test surface.

The heat transfer test section flush mounts in a specially constructed flat plate which is located in an open surface water channel (see Figure 9). The plate allows initial development of a flat plate laminar or tripping to give a turbulent boundary layer, prior to the flow passing over the heated test plate. Vortex generating devices can be affixed to the flat plate to generate a variety of vortex configurations of interest, including end-wall necklace and horseshoe vortices for bluff bodies ranging from cylinders to airfoils, hairpin vortices using hemispherical protuberances and slot injection, and turbulent spot generation using slot injection.

Flow visualization using hydrogen bubbles, particle imaging, and thermochromic liquid crystal heat transfer visualization is viewed and recorded using a Sony broadcast grade three-chip color camera with ultra zoom lens, and a Panasonic broadcast grade S-VHS recorder, with lock-in variable slow motion and freeze frame capability; viewing is done on a SONY 19", 700 line color monitor. Both the camera and recording system can be interfaced to a Data Translation color image grabber, image analysis system with accelerator card, and image convertor for operation in HSI (Hue-Saturation-Intensity) space. The image analysis system is supported by a Gateway 486-66 computer, with off-loading capability to a MacIntosh IIvx computer with state-of-the-art image analysis software. This combined computer system allows color images to be rapidly interrogated for color (hue) distribution, converting the hue values to calibrated temperature values in the heat transfer study. Conventional hydrogen bubble images can also be evaluated for quantitative behavior, and a PIV imaging system (described below) allows displacement/velocity information to be acquired. This image analysis system is a very versatile and somewhat unique system which unfortunately took over six months to get running properly. After much effort to overcome hardware and software problems, the system is functioning very effectively, as will be illustrated below.

A support/traverse system for miniature thermocouple probes has been constructed and tested. The traverse system allows location of the probes within 25 μm increments. The thermocouple probe allows local temperature measurements to be made in the water flow region immediately adjacent to the heated surface and facilities examination of temporal changes in the mass transport of heated fluid by vortex interactions, which allows the correlation of the surface heat transfer with thermal

transfer within the flow field by the respective vortex structures. Initial studies have been conducted with Fe-Cn thermocouples constructed from 80 μm wires, and indicate a frequency response in excess of 100 Hz, again quite acceptable for the low-speed vortex flows under examination. The input data from the thermocouple is fed directly to a separate 486-66 data acquisition computer, which allows spatial-temporal temperature patterns using a second surface-mounted thermocouple as a phase reference signal.

During the second year of the contract, a 10-watt LEXEL Argon Laser was purchasd and integrated into the visualization system to provide scanned laser sheet illumination for particle and hydrogren bubble flow visualization, and for scanned PIV image acquisition. The Laser has been installed and the optics for creating a scanned illumination light sheet were developed. Because of the low speeds and the small scales of the necklace and hairpin vortices employed in the studies, a scanned beam approach, with adjustable beam sweep has been employed for particle visualization studies (see below); however, a 72 facet, rotating mirror has proved most effective for acquisition of PIV images. In a subsequent contract, a 144 facet mirror will be implemented, which will provide a smaller field of view, increased local illumination, and a higher scanning rate, all of which will increase our capabilities for small-scale PIV studies.

Although a very time consuming process, all major experimental systems have been developed and been in place for about eight months. Employing these systems, detailed studies of both vortex dynamics and surface heat transfer have been pursued over the past year; a summary of these studies is presented in the following sections.

3.3.2 Dynamics of End-Wall Vortices

Detailed experimental examination of end-wall vortex behavior during the two-year grant period has revealed several aspects of vortex formation/behavior in the end-wall region which have not been previously observed and understood. In particular, a systematic examination of the unsteady necklace vortex formation process, mentioned in the Introduction above, has shown that the formation process is precipitated by the interaction of the strong adverse pressure gradient in the approach flow region with the impinging boundary layer on the flat plate surface. The magnitude and distribution of this pressure gradient is a key parameter in establishing when the necklace vortices will begin an unsteady, periodic formation process. It has also been established that the frequency of vortex formation within this periodic regime depends primarily on the vorticity flux of the incident boundary layer, U^2/ν, and the boundary layer Reynolds number, Re_{δ^*}, with the cylinder or bluff body Reynolds number, Re_D, having only a secondary influence (Smith, Greco, and Fitzgerald, 1993).

Examination of the initial pattern of formation of the necklace vortices within the initial stable regime has confirmed the results of Visbal (1991) that the streamline/separation pattern in the approach region may display either an initial point of surface separation (the conventional "jet maze" pattern), or an unusual point of surface attachment, with the separation point moving aloft from the plate as a saddle point. Fitzgerald (1993) shows that the necklace system passes through three regimes of behavior, over which the outermost critical point changes from a point of surface separation to a point of attachment. The impact of this shift in behavior on the surface heat transfer is expected to be quite pronounced.

To facilitate our understanding of the quantitative behavior of unsteady juncture flows, a PIV study was undertaken of the spatial-temporal velocity-vorticity field on the symmetry plane of a laminar, rectangular block-flat plate juncture (Seal, 1993). A

rectangular geometry was examined since it provides a very stable and repeatable periodic necklace vortex system. A digitized image of the general appearance of a temporal flow pattern visualized using hydrogen bubbles is shown in Figure 10. Sequential particle image pictures for this flow pattern were obtained on the symmetry plane of the flow using 12 μm metallic coated particles in a concentration of 1.7×10^6 particles per gallon of water. The location and dimensions of the region examined are shown in Figure 11, in conjunction with the instantaneous streamlines for one temporal realization, illustrating the quantitative presence of the two necklace vortices shown in Figure 10. Employing the 84×54 vector array obtained from each realization, the vorticity field was numerically derived; Figure 12a illustrates the vorticity contours for a sequence of temporal realizations, illustrating the periodic propagation of the necklace vortices toward the juncture, and the subsequent amalgamation of the vortices, and their corresponding vorticity, in the corner region, yielding a periodically re-energized corner vortex. Analysis of the details of the vorticity and vortex strength for both this sequence, and a sequence with a turbulent approach flow (reported in Seal, 1993) have been done to establish the interaction characteristics of the necklace vortices both with themselves and in generating opposite-sign vorticity at the surface. In general, the necklace vortices are observed to generate significant regions of concentrated opposite sign vorticity through interaction with surface fluid, which is ejected from the surface and interacts with the necklace vortex, thus diminishing its strength. These types of opposite sign vorticity concentrations appear clearly in Figure 12a (note particularly the next-to-last realization in the sequence). Further examination of the vorticity field reveals that the vorticity flux in the x direction (Figure 12b) varies significantly, with the convected vorticity concentrating into the necklace vortices (indicated by the negative valleys in the flux), which are transported toward the block. Note that the magnitude of these valleys diminishes as the block is approached, indicating a significant reduction in vortex strength due to interaction of the necklace vortices with the induced opposite sign vorticity.

Work is continuing on understanding end-wall vortex dynamics, particularly the temporal regime, since this will help in understanding the processes inherent in the turbulent regime, which will be examined extensively in the flollow-on grant. Initial studies of the turbulent regime, with a turbulent approach flow, indicate that the vorticity inducing vortex-surface interactions play an extremely important role in the behavior of turbulent junction vortices, and have clear implications on the processes responsible for junction surface heat transfer. In general, in the turbulent regime vorticity generation develops as localized opposite-sign vortices, which suddenly focus and erupt from the surface (Doligalski, Smith, and Walker, 1994) essentially identical to the process suggested by the computational studies. The significance of these eruptive characteristics will be explored in detail in the follow-on studies.

3.3.3 Heat Transfer Studies

Heat transfer studies using the liquid crystal test surface have now been done for both end-wall vortices and a tripped turbulent boundary layer. The surface now works extremely well, although a good deal of time was required to develop effective and repeatable techniques for painting the liquid crystal surface on the foil heater. The surface yields very distinct color patterns, reflective of the temperature distribution, with a response time in the 8 to 10 Hz range. However, acquisition of the color patterns could not be done effectively with a standard CCD color camera. This required the purchase of a 3-chip CCD camera, which feeds separate RGB signals to the digitizer. This addition has allowed the acquisition of quality color images, which are then converted to HSI space. The hue buffer (H) of these images, which contains the true

color information, is the buffer that is calibrated and interrogated to establish the surface temperature distribution. Once the images are calibrated, they can be displayed as a new color or grain level image reflective of the temperature patterns. These patterns are evaluated, both as dynamic sequences, and statistically for property data. Figure 13a is a gray level image of the surface temperature pattern for a laminar approach flow to an airfoil juncture. Note the light "rings" which clearly engirdle the leading edge of the airfoil (the black region to the right of Figure 13a). These rings are the clear indication of a systematic decrease in local temperature due to increased heat transfer in the juncture region due to the presence of the unsteady necklace vortices, substantiating the findings of the computational studies (see Section 3.1). Figure 13b, a 3-D plot of the surface temperature shown in Figure 13a, reinforces the strong variations present in this region. When viewed dynamically, either in the original images or the processed temperature distributions, the very sharp color changes reflective of surface temperature variations are observed to move in concert with the movement of the periodic necklace vortices. Figure 14 is a 9-image sequence of temporal surface temperature variations over the period of formation for a periodic, unsteady necklace vortex system similar to that shown previously in Figure 10. In this figure the image has been displaced in 5 gray levels, with each level reflective of a 1°C temperature variation, with light indicating the highest temperature and dark the lowest. Evaluations of the heat transfer coefficient indicate that the necklace vortices can result in temporal variations of as much as $\pm 50\%$ in the local heat transfer coefficient.

Similar results have been obtained for the surface heat transfer response to a tripped, turbulent boundary layer, as shown in Figure 15. This figure illustrates the presence of spanwise surface temperature "streaks" which are clearly associated with the classic turbulent boundary layer low-speed streaks. Similar studies by Iritani et al. (1984) (see also Kasagi et al., 1989) have shown the presence of such structures, however, previous works did not have a surface of sufficient response to appropriately track the temporal temperature variations. The present surface has the response characteristics necessary to establish the inherent influence of vortices within near-wall turbulence on surface heat transport. Presently, work is continuing to develop methods for correlation of particle image visualizations of the vortex structure with both the surface temperature patterns and the phase-correlated temperature patterns within the fluid. Once this process of data/pattern correlation is refined for the simpler vortex systems, the techniques for establishing the interrelationship between vortices and spatial-temporal heat transfer will be extended to fully turbulent flows. In addition, further refinement of the process of image acquisition is continuing, and extension of the surface heat transfer study to other characteristic vortex structures are being pursued under the follow-on grant.

3.4 References

Cowley, S. J., Van Dommelen, L. L. and Lam, S. T. 1991 On the Use of Lagrangian Variables in Descriptions of Unsteady Boundary Layer Separation", *Philosophical Transactions of the Royal Society of London A* 333, pp. 343-378.

Doligalski, T. L., Smith, C. R., and Walker, J. D. A. 1993 "Vortex Interactions with Walls", *Annual Review of Fluid Mechanics* (in press).

Fitzgerald, J. P. 1993 "Critical Points of Separation and Attachment in the Steady, Three-Vortex System for a Flat Plate-Cylinder Juncture", M. S. Thesis, Department of Mechanical Engineering and Mechanics, Lehigh University.

Greco, J. J. and Smith, C. R. 1991 "The Flow Structure in the Vicinity of a Cylinder - Flat Plate Junction: Flow Regimes, Periodicity and Vortex Interactions", Report FM-18, Department of Mechanical Engineering and Mechanics, Lehigh University, Bethlehem, Pennsylvania

Smith, C. R., Greco, J. J., and Fitzgerald, J. P. "The Flow Structure in the Vicinity of a Cylinder - Flat Plate Junction: Flow Regimes, Periodicity and Vortex Interactions", Report FM-18, Department of Mechanical Engineering and Mechanics, Lehigh University, Bethlehem, Pennsylvania.

Haidari, A. H. and Smith, C. R. 1984 "A Cooperative Study of the Development of the Turbulent Near-Wake Behind a Thick Flat Plate with Both a Circular and Trailing-Edge Geometry", Report FM-6, Lehigh University, Bethlehem, Pennsylvania.

Hung, C. M., Sung, C. H. and Chen, C. L. 1991 "Computation of Saddle Point of Attachment", AIAA Paper 91-1713.

Iritani, Y., Kasagi, N., and Hirata, M. 1984 "Heat Transfer Mechanism and Associated Turbulence Structure in Near-Wall Region of a Turbulent Boundary Layer", Turbulent Shear Flows 4 (ed. L. J. S. Bradbury, F. Durst, B. E. Launder, F. W. Schmidt, and J. H. Whitelaw), Springer-Verlag, Berlin, pp. 223-234.

Kasagi, J., Mofatt, R. J. and Hirata, M. 1989 "Liquid Crystal", Chapter 8 in Handbook of Flow Visualization (ed W. J. Yang), Hemisphere Publishing, Washington, D. C., pp. 105-124.

Seal, C. V. 1993 "The Flow Regimes and Velocity Field at a Rectangular Block-Flat Plate Juncture with a Laminar Approach Flow", M. S. Thesis, Department of Mechanical Engineering and Mechanics, Lehigh University.

Smith, C. R., Walker, J. D. A., Haidari, A. H. and Sobrun, U. 1991 "On the Dynamics of Near-Wall Turbulence", *Philosophical Transactions of the Royal Society of London A* 336, pp. 131-175.

Visbal, M. R. 1991 "On the Structure of Laminar Juncture Flows", *AIAA Journal* (to appear).

4. ASSOCIATED PUBLICATIONS, PRESENTATIONS, THESES
(During the present AFOSR contract period)

4.1 Publications

4.1.1 Smith, C. R., Fitzgerald, J. P., and Greco, J. J., "Cylinder End-Wall Vortex Dynamics", *Physics of Fluids A*, Vol. 3, No. 9, p. 2031, 1991.

4.1.2 Smith, C. R., Walker, J. D. A., Haidairi, A. H., and Sobrun, U., "On the Dynamics of Near-Wall Turbulence", *Philosophical Transactions of the Royal Society of London A*, 336, pp. 131-175, 1991.

4.1.3 Walker, J. D. A. and Smith, C. R., "Dynamics of the Turbulent Wall Layer", Proceedings of AFOSR Contractors Workshop on Turbulence Structure and

Control, T. Herbert, ed., Ohio State University, April 1991, pp. 24-28.

4.1.4 Smith, C. R. and Walker, J. D. A., "Vortex Interactions in the End-Wall Boundary Layer", Proceedings of AFOSR Contractors Workshop on Turbulence Structure and Control, T. Herbert, ed., Ohio State University, April 1991, pp. 24-28.

4.1.5 Doligalski, T. L., Smith, C. R., and Walker, J. D. A., "Vortex Interactions with Walls", *Annual Review of Fluid Mechanics* (in press).

4.1.6 Smith, C. R. and Walker, J. D. A., "Turbulent Wall-Layer Vortices", Chapter in Fluid Vortices (ed. S. Green, Hemisphere) (in press).

4.1.7 Puhak, R., Degani, A. and Walker, J. D. A., "Unsteady Separation and Heat Transfer in an Upstream of Obstacles", *Journal of Fluid Mechanics* (in review).

4.1.8 Smith, C. R., Greco, J. J., and Fitzgerald, J. P. "Necklace Vortex Formation for a Circular Cylinder: Flow Regimes, Frequency Scaling, and Topology", *Journal of Fluid Mechanics* (in review).

4.1.9 Seal, C. V., Smith, C. R., Akin. O. and Rockwell, D., "Instantaneous Velocity and Vorticity Characteristics in the Juncture Region of a Rectangular Block-Flat Plate", *Journal of Fluid Mechanics* (in review).

4.2 Theses in Progress (expected completion date)

4.2.1 Fitzgerald, J. F., "Critical Points of Separation and Attachment in the Steady, Three-Vortex System for a Flat Plate-Cylinder Juncture", M. S. Thesis (June 1993).

4.2.2 Ianonne, L. A., "Self-Similar Heat Transfer Solutions in Three-Dimensional Flows", M. S. Thesis (December 1992).

4.2.3 Seal, C. H., "The Flow Regimes and Velocity Field at a Rectangular Block-Flat Plate Juncture with a Laminar Approach Flow", M. S. Thesis (December 1992).

4.2.4 Puhak, R., "Heat Transfer and Separation in End-Wall Boundary Layers", Ph.D. Thesis (December 1993).

4.2.5 Takmaz, L., "An Evaluation of the Time-Dependent Surface Heat Transfer Due to Transient End-Wall Vortices", Ph.D. Thesis (January 1994).

4.2.6 Demir, M., "Heat Transfer Due to Vortex-Induced Separation", M.Sc. Thesis (December 1992).

5. PERSONNEL

5.1 Co-Principal Investigators

C. R. Smith, Professor of Mechanical Engineering

J. D. A. Walker, Professor of Mechanical Engineering

5.2 Student Research Assistants

		Completion Date
R. Puhak	Ph.D. Candidate	June 1993
L. Takmaz	Ph.D. Candidate	January 1994
M. Demir	M.S. Candidate	December 1992
L. A. Iannone	M.S. Candidate	December 1992
J. P. Fitzgerald	M.S. Candidate	June 1993
C. H. Seal	M.S. Candidate	June 1993

6. INTERACTIONS

6.1 Presentations

6.1.1 C. R. Smith

"Vortex Interactions in the End-Wall Boundary Layer", AFOSR Contractors Workshop on Turbulence Structure and Control, Columbus, Ohio, 1 April 1991.

"Temporal End-Wall Vortex Behavior: An Illustration of Pressure Gradient Induced Transition", McDonald-Douglas Research Laboratories, St. Louis, Missouri, 1 May 1992.

"The Development of Flow Structure in End-Wall Boundary Layers: A Metamorphosis of Three-Dimensional Unsteady Vortex Behavior", Invited Paper, Conference on Turbulent Flows in Honor of S. J. Kline Retirement, Stanford, CA, 10 August 1992.

"Flow Structure and Transition in Wall Junction Region", Invited Seminar, NASA Langley Flow Physics Branch, Langley, VA, 19 September 1992.

"Surface Heat Transfer Due to Unsteady End-Wall Vortex Flow Structure", 45th Meeting of American Physical Society, Tallahassee, FL, 24 November 1992.

"Use of Kernel Experiments for Modeling of Near-Wall Turbulence", International Conference on Near-Wall Turbulent Flows, Tempe, AZ, 15 March 1993.

"The Dynamics of Wall Turbulence: The Importance of Vortex Interactions", Invited Seminar, Naval Underwater Weapons Center, New Port, RI, 15 April 1993.

6.1.2 J. D. A. Walker

"Dynamics of Turbulent Wall Layers", Rutgers University, April 1, 1992.

"Unsteady Two-Dimensional Separation", AFOSR Workshop on Super-maneuverability, Lehigh University, April 9-10, 1992.

"Unsteady Separation and Heat Transfer Upstream of Obstacles", 45th Meeting of American Physical Society, Tallahasse, FL, November 24, 1993.

"Aspects of Turbine Blade Heat Transfer", AFOSR/ONR Contractor Meeting, Chicago, IL, June 10-12, 1992.

"Aspects of Unsteady Separation", Invited Talk, AFOSR Symposium on Computational Fluid Dynamics, Wright Patterson AFB, Dayton, OH, September 15-16 1992.

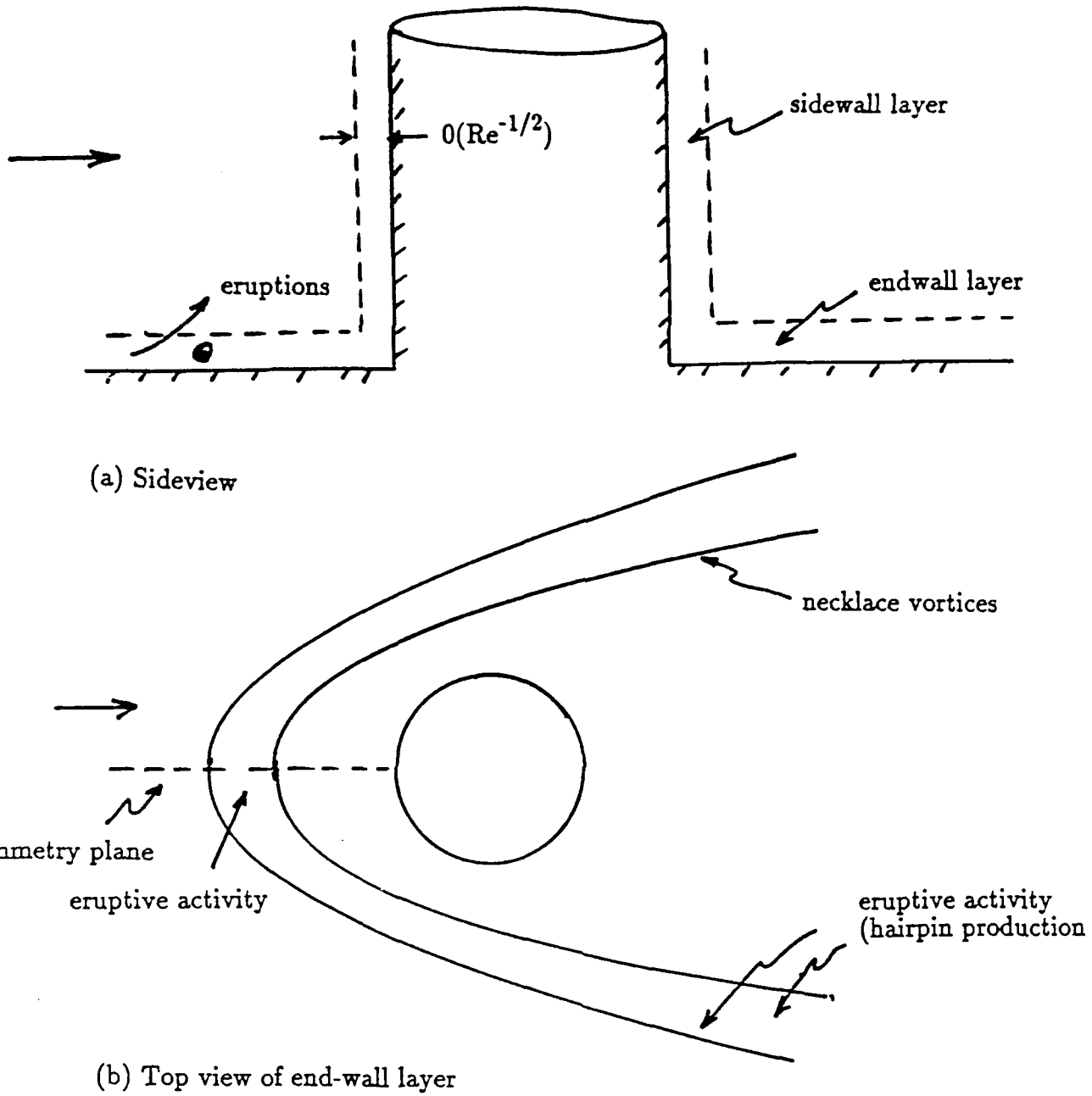

Figure 1. Schematic diagram of a model juncture flow showing locations where unsteady separation initiates.

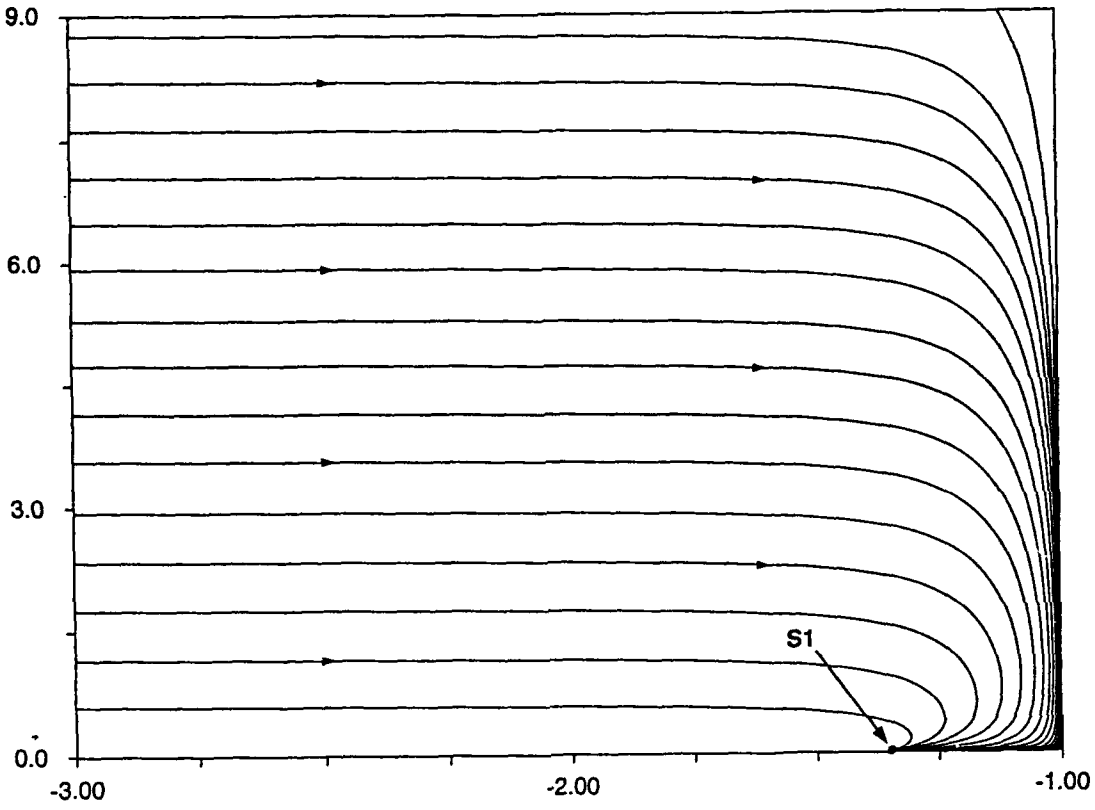

(a) $t = 1.0$

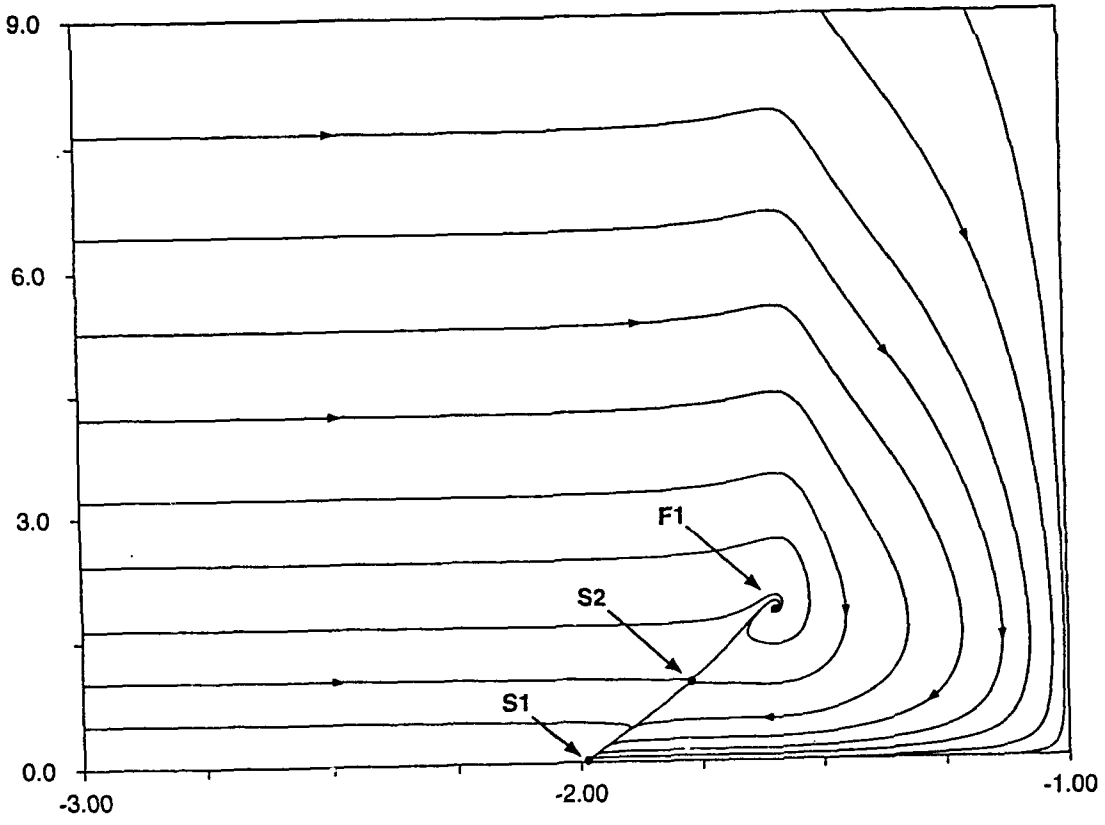

(b) $t = 3.5$

Figure 2. Calculated streamline patterns on the symmetry plane of an end-wall boundary layer following an impulsive start.

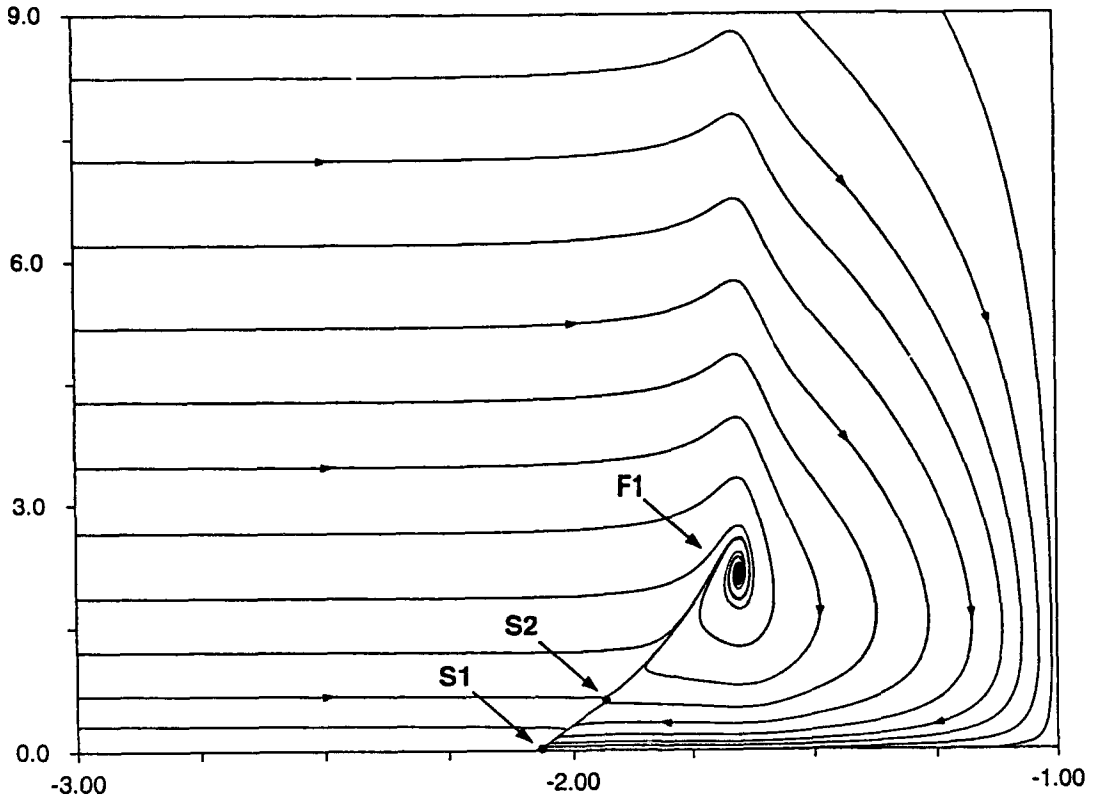

(c) t = 4

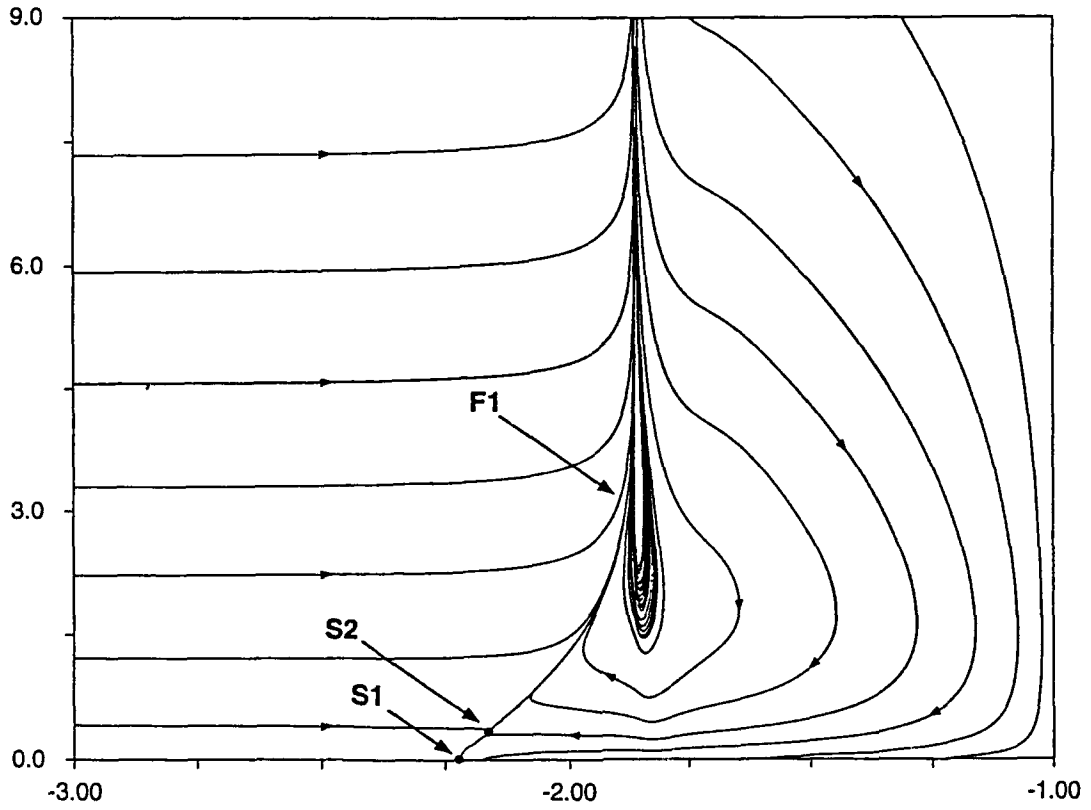

(d) t = 5.2

Figure 2. Continued.

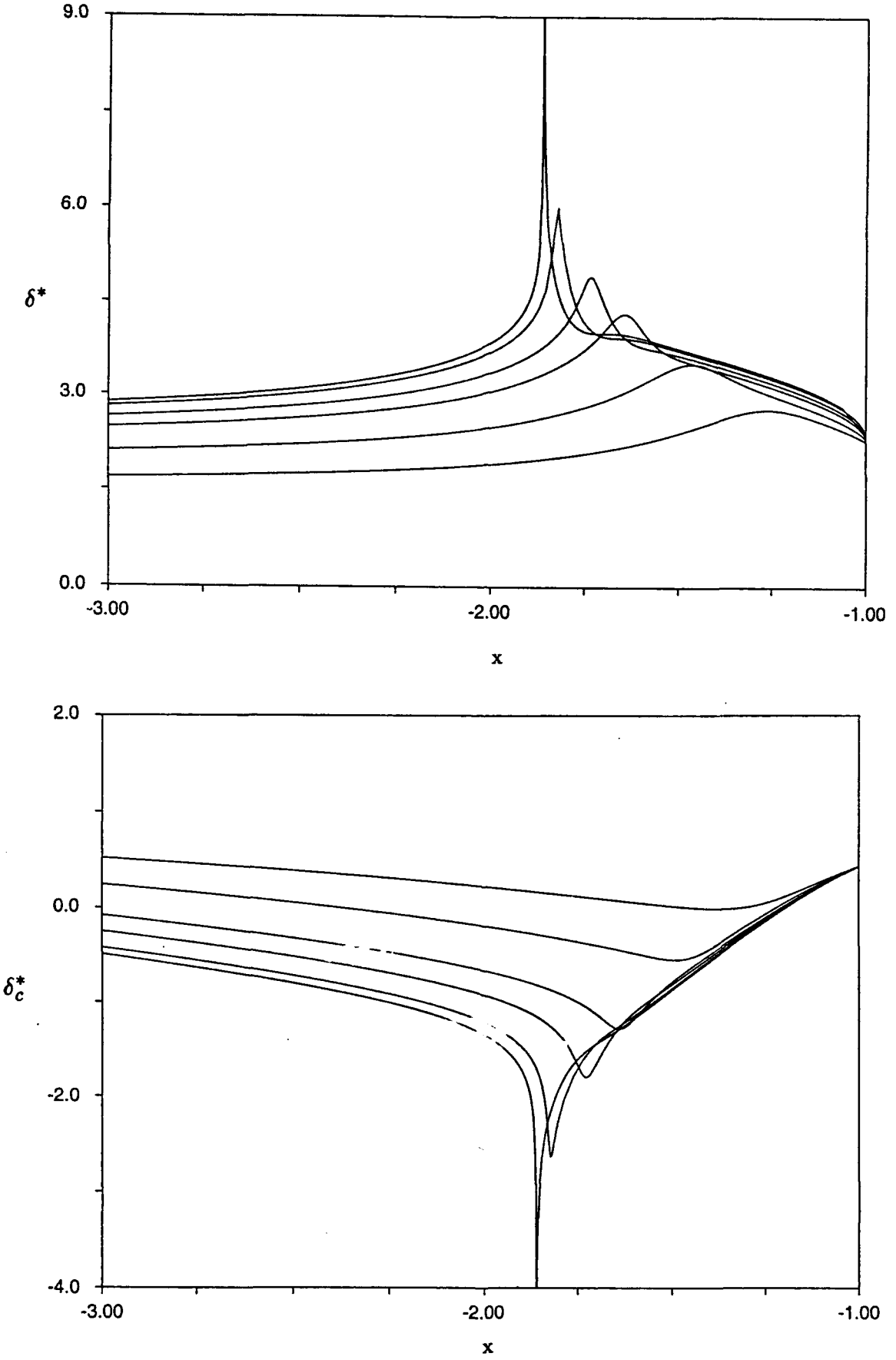

Figure 3. Temporal development of (a) displacement thickness and (b) cross-stream displacement thickness. Plotted curves are at t = 2.0, 3.0, 4.0, 4.5, 5, and 5.2.

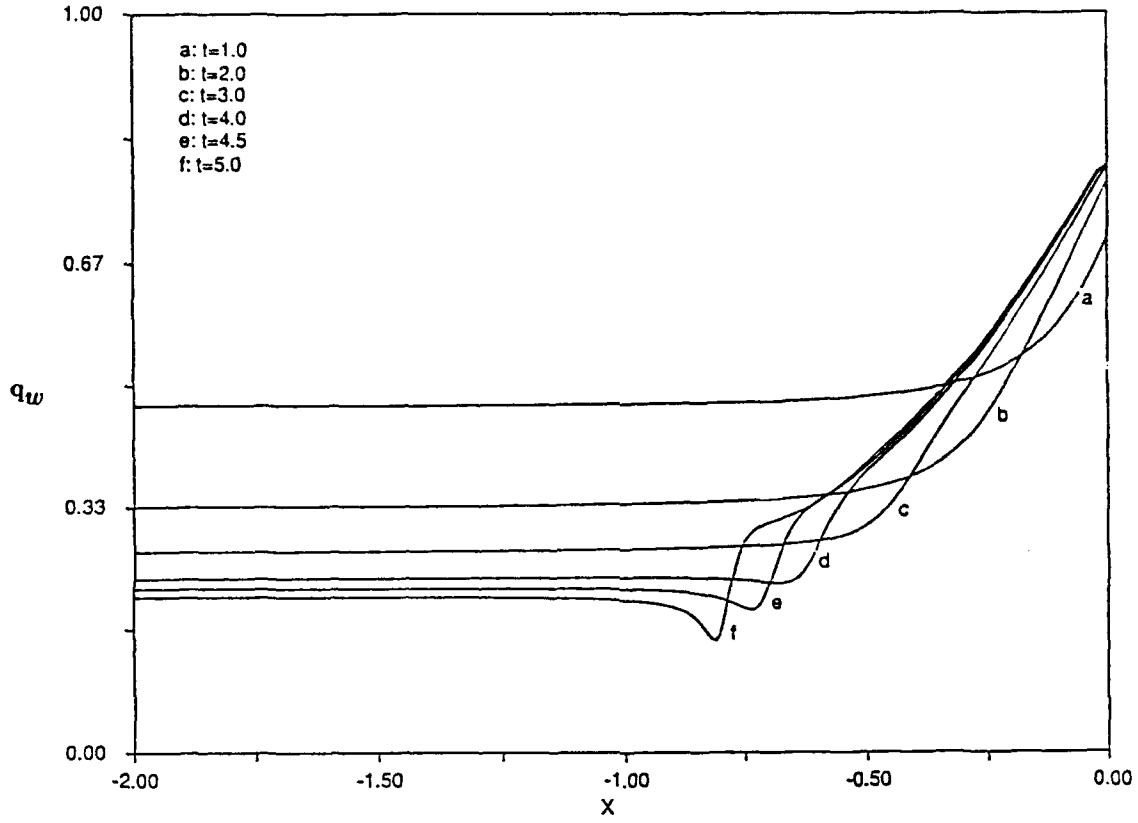

(a) surface heat flux

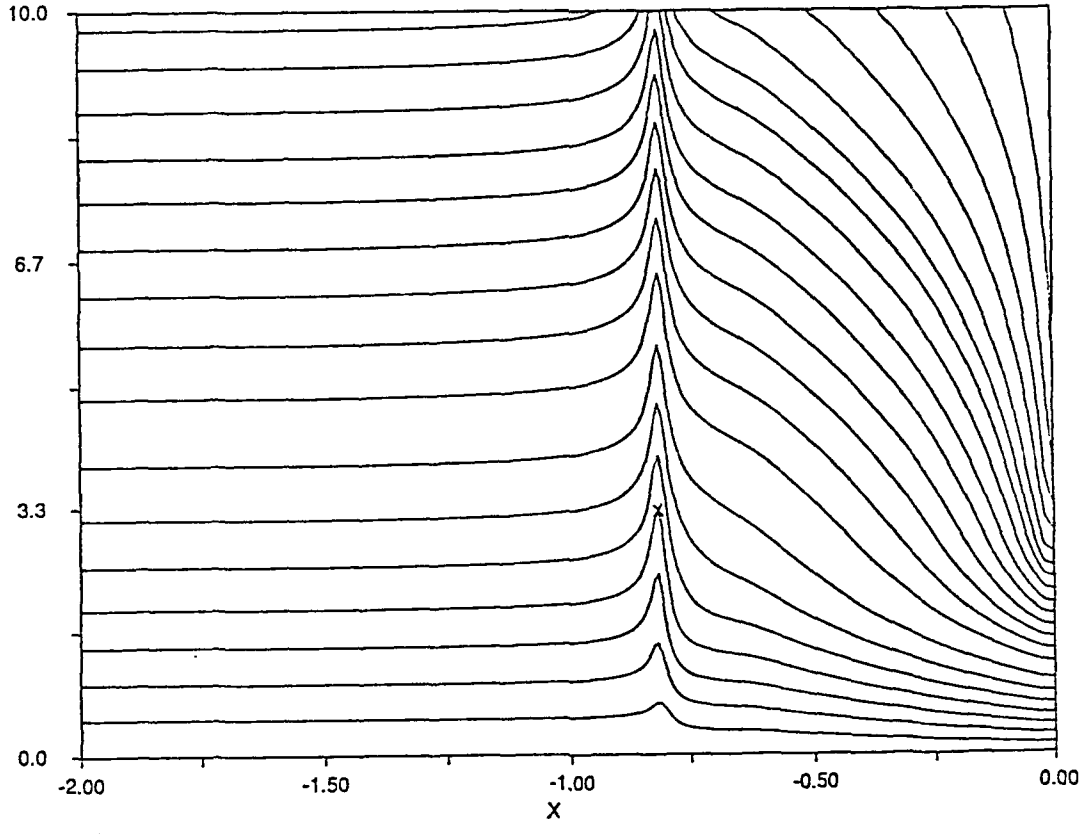

(b) contours of constant temperature at t_s

Figure 4. Temporal development of the surface heat flux and temperature field at t_s.

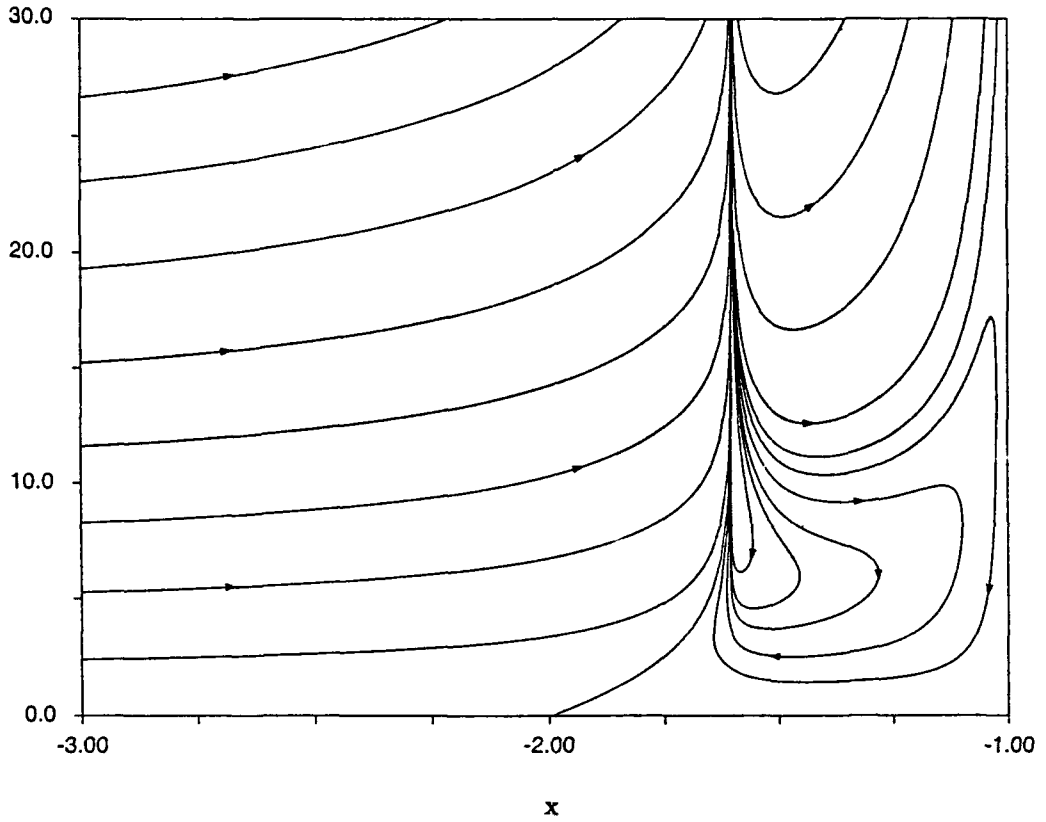

Figure 5. Instantaneous streamlines at separation for the two-dimensional obstruction.

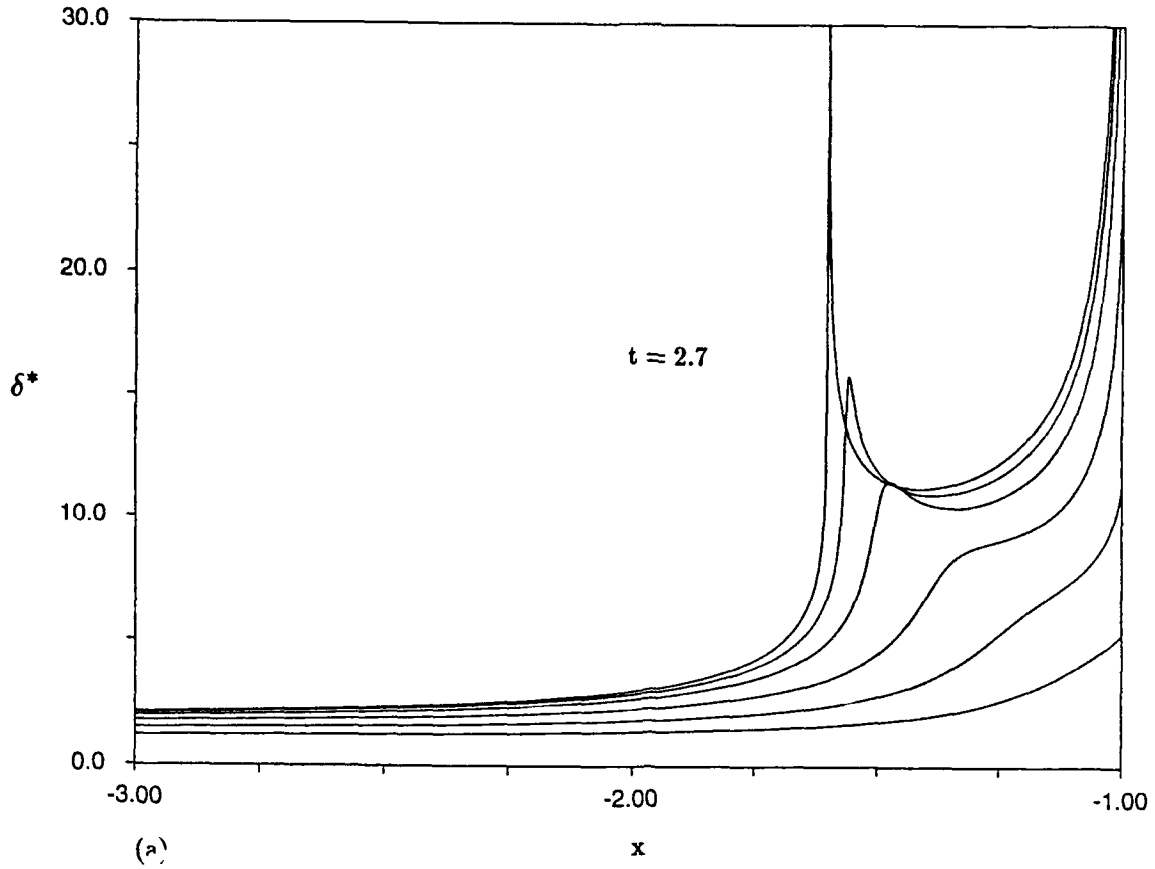

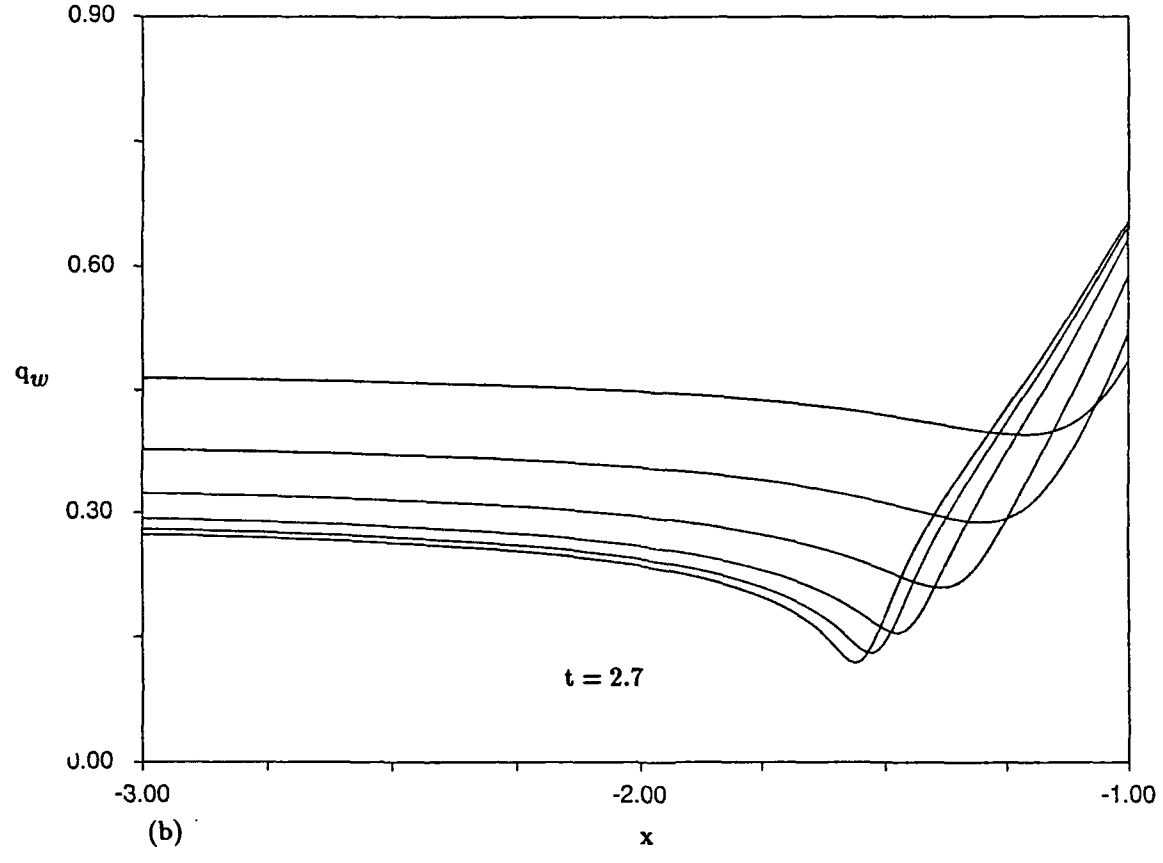

Figure 6. Temporal evolution of (a) displacement thickness and (b) wall heat flux. Plotted curves are at t = 1.0, 1.5, 2.0, 2.4, 2.6 and 2.7.

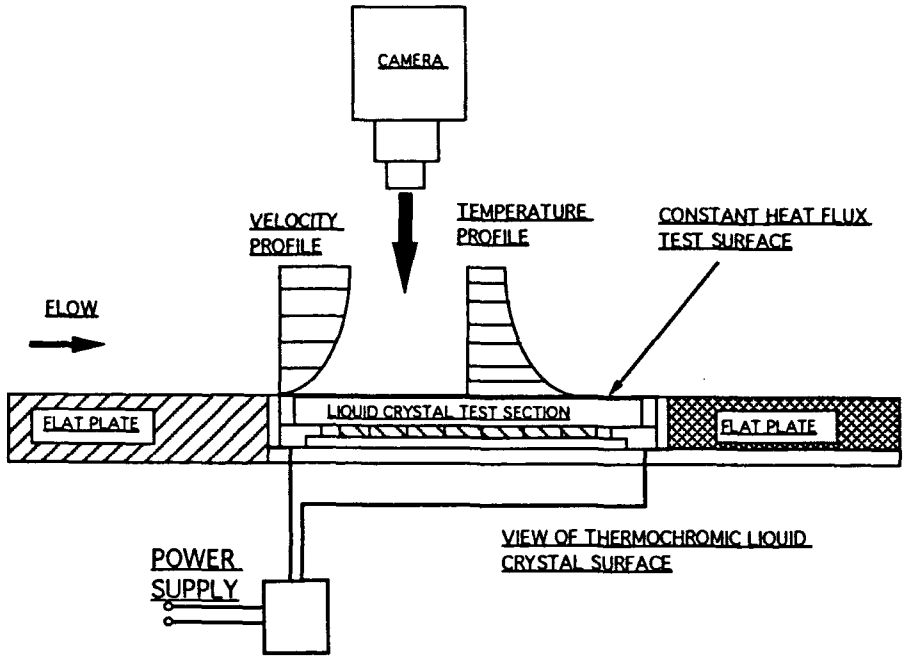

Figure 7. Constant heat transfer test section illustrating flush mounting in flat plate. Note viewing of thermochromic liquid crystal surface from above through the channel surface.

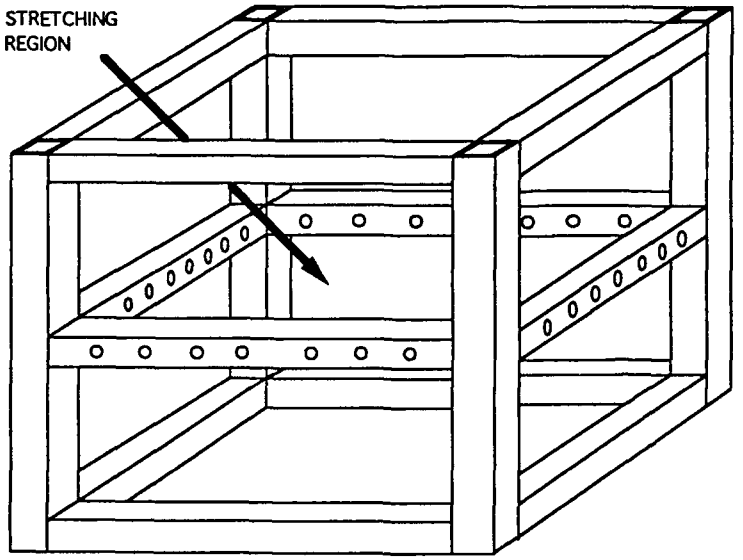

Figure 8. Tubular steel frame for stretching stainless steel heating foil.

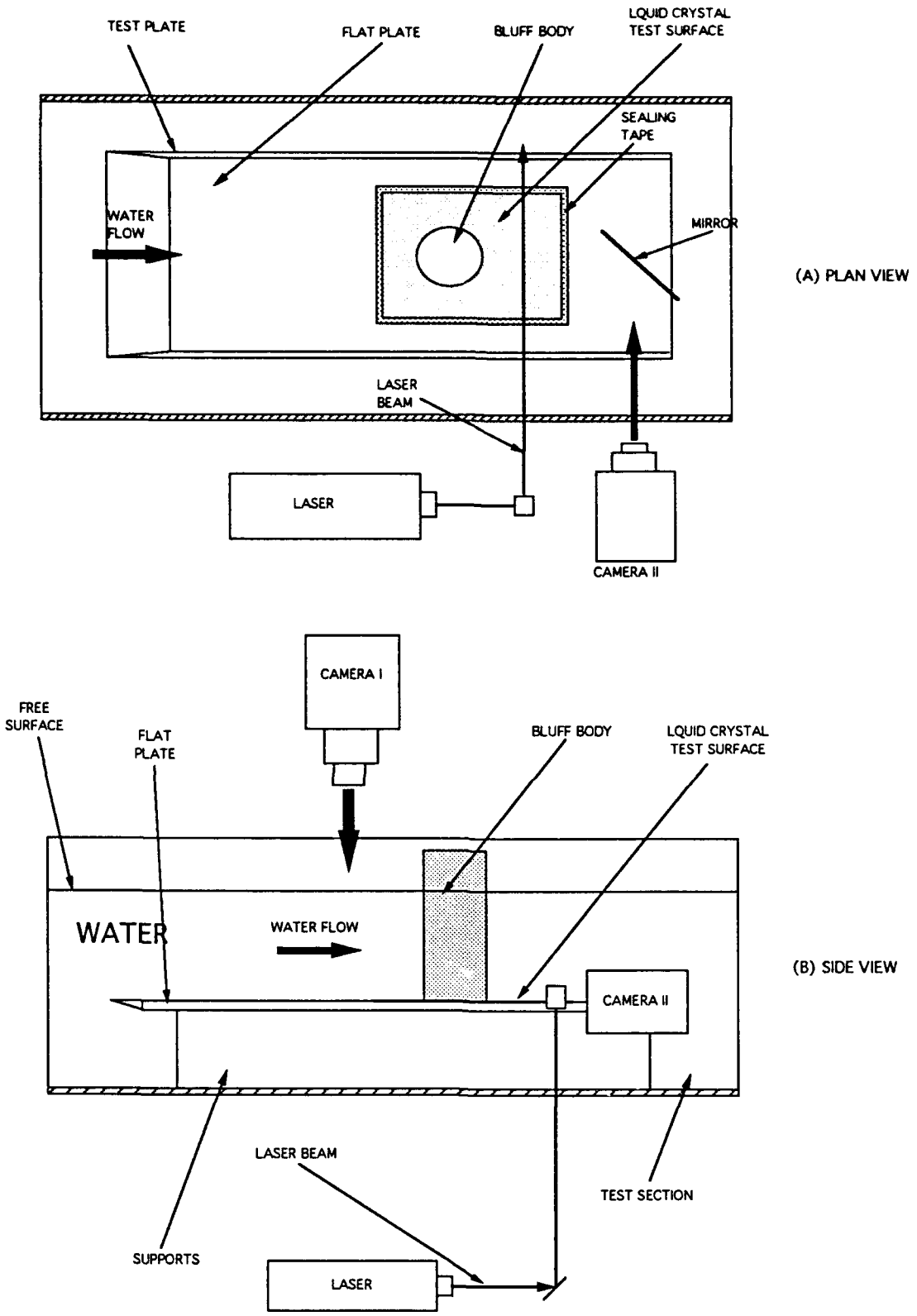

Figure 9. Flat plate test section with liquid crystal (constant heat flux) test section flush-mounted in plate. *Note* the arrangement of the two viewing cameras and laser lighting system.

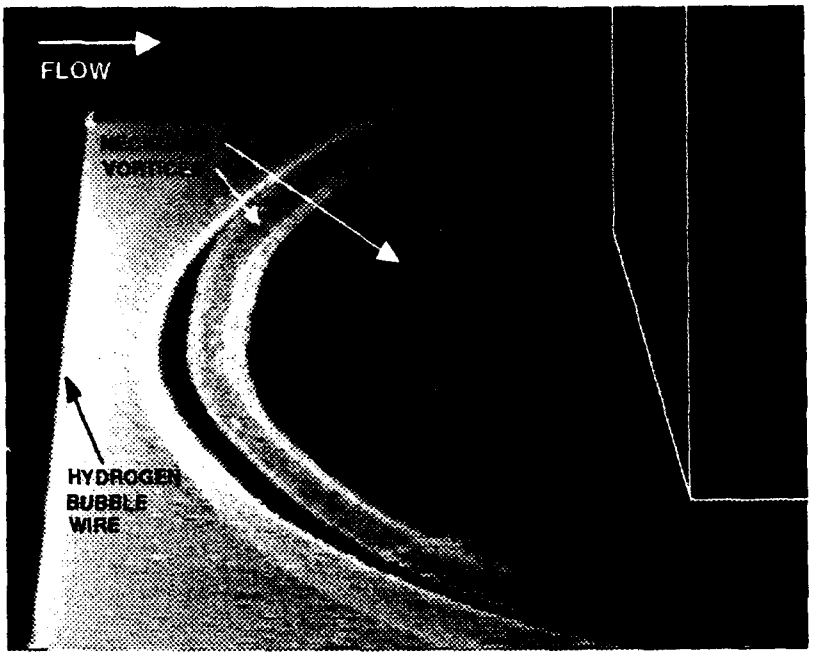

Figure 10. Hydrogen bubble visualization of the periodic necklace vortex system at a rectangular block-flat plate juncture.

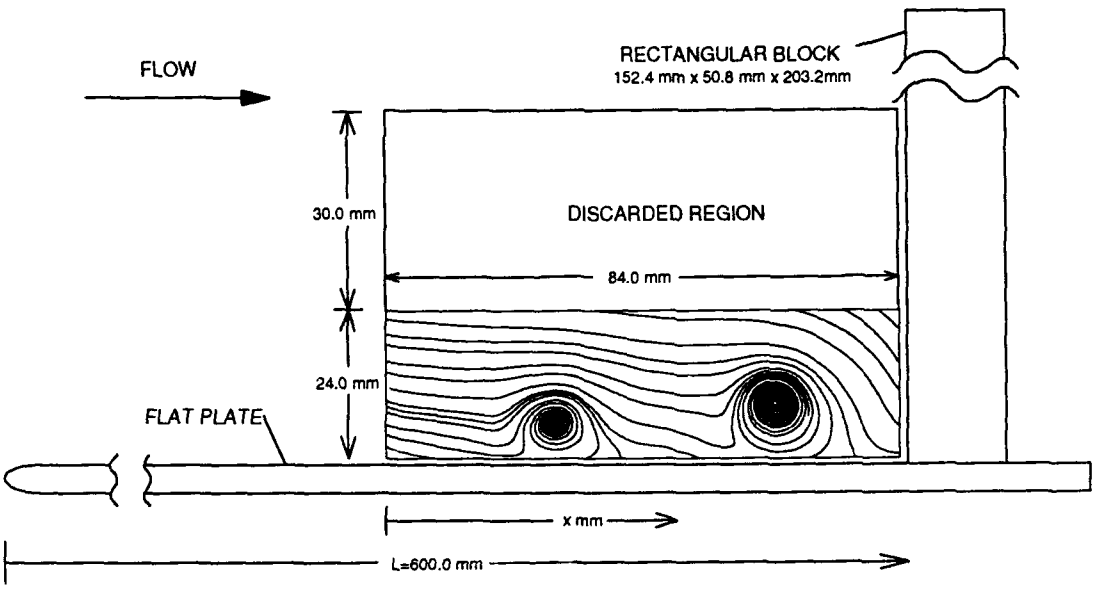

Figure 11. General location of the rectangular block on the flat plate test section illustrating a typical streamline pattern for the flow shown in Figure 10.

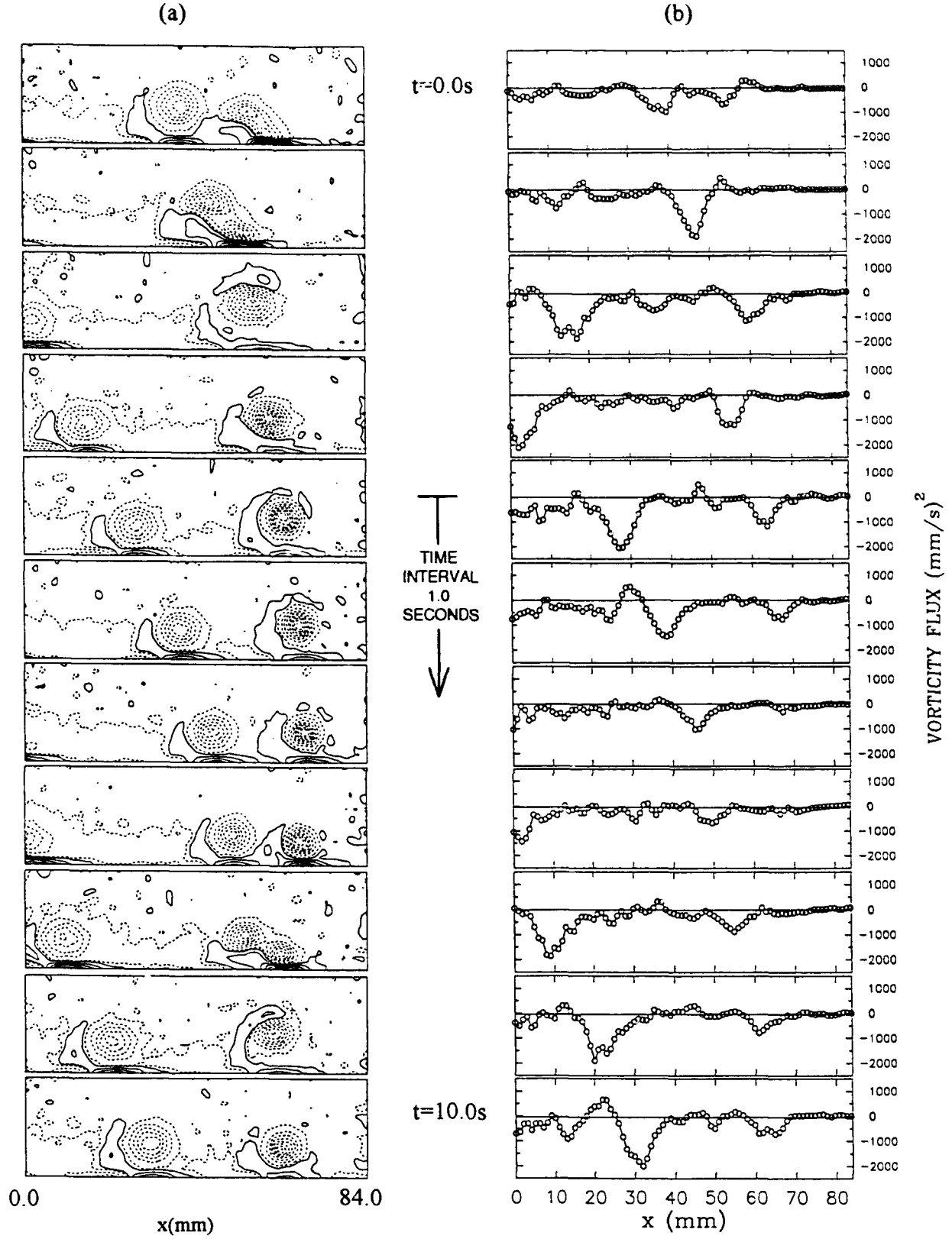

Figure 12. An eleven realization sequence of (a) isovorticity contours (positive: solid lines, negative: dashed lines), and (b) vorticity flux for periodic flow in a rectangular block-flat plate juncture. Flow is left-to-right, with block at x = 84 mm; each realization is one second apart.

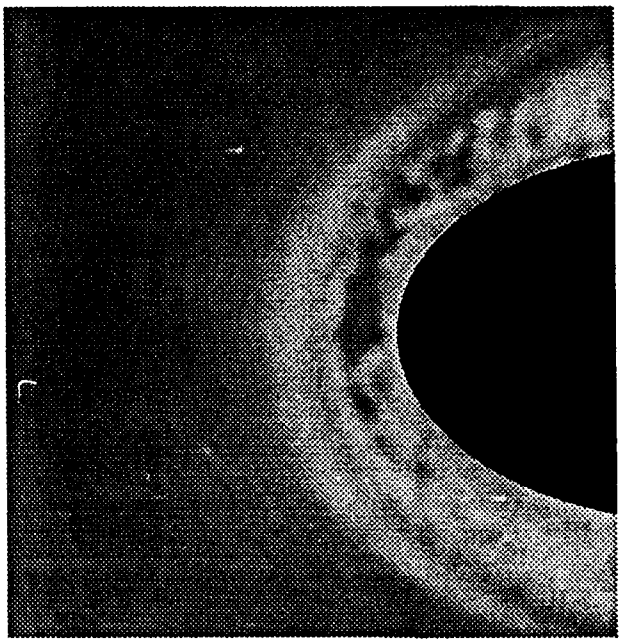

(a) Plan-view, Grayscale image of temperature pattern

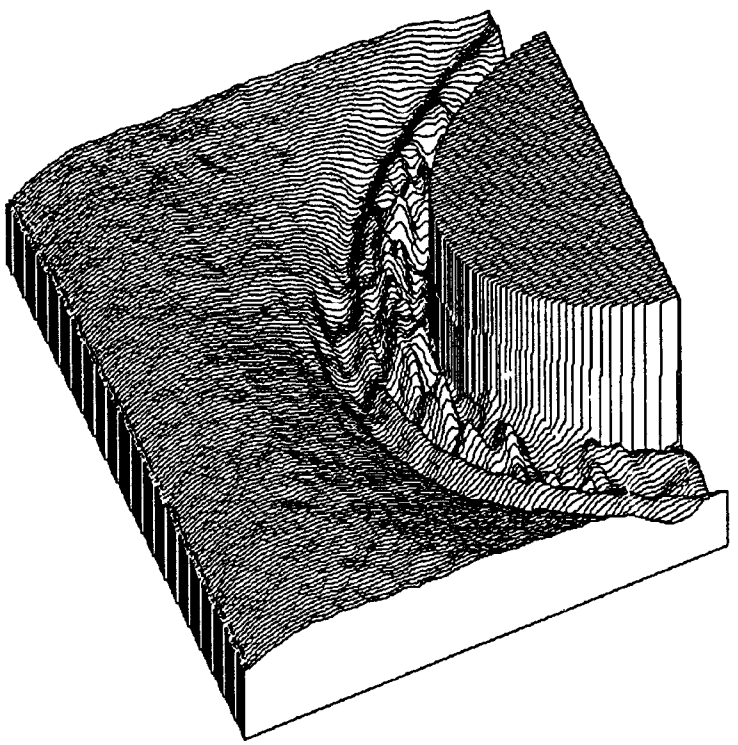

(b) 3-D plot of surface temperature distribution of (a)

Figure 13. Examples of the instantaneous temperature pattern on a constant heat transfer surface created by periodic necklace vortices at a flat plate-air foil juncture.

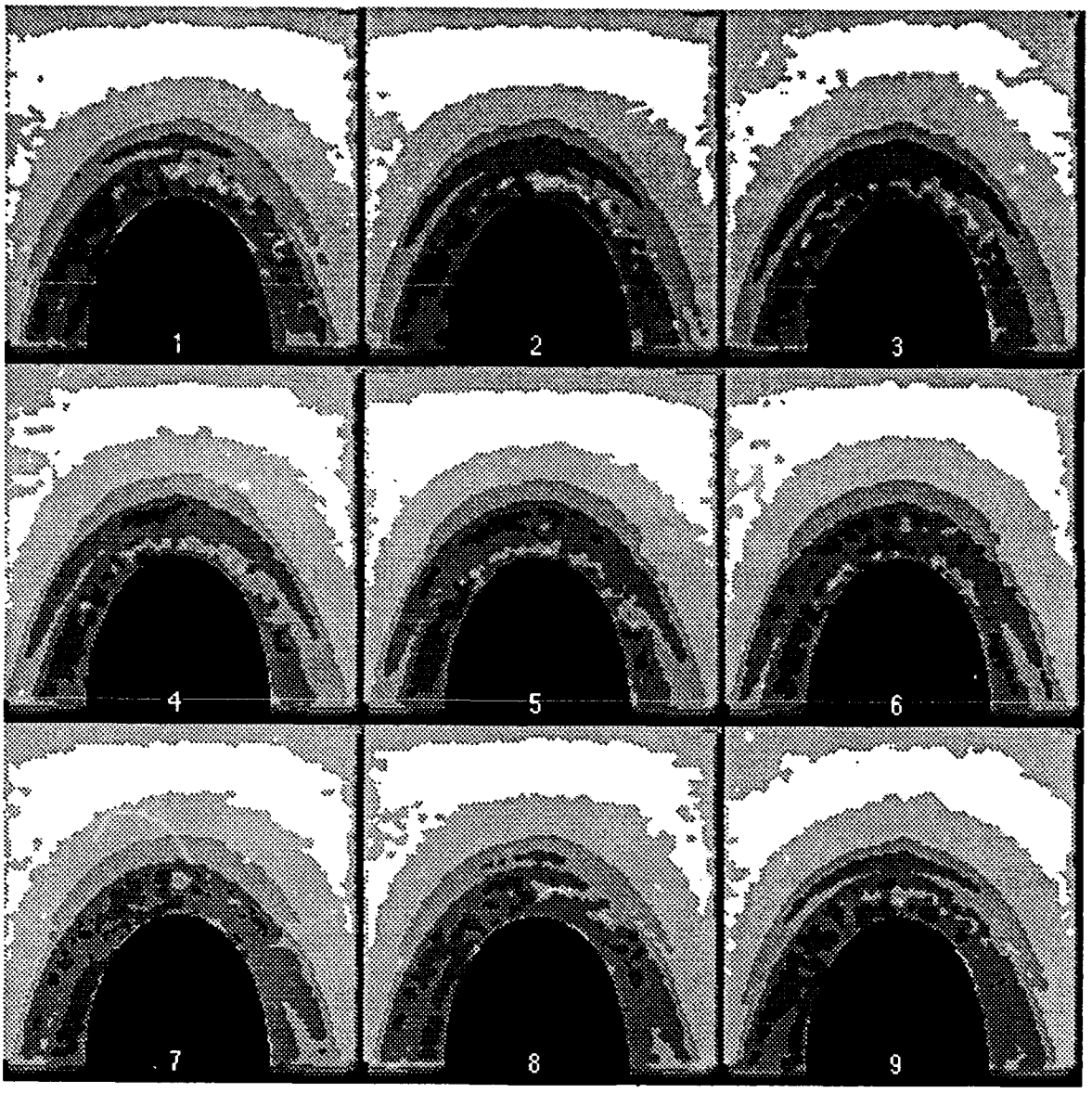

Figure 14. Sequential surface temperature variations induced by the periodic generation and migration of necklace vortices around a flat plate-airfoil juncture. Flow is top-to-bottom with $Re_t = 8000$. Each gray-level indicates a 1°C temperature change; each picture is 0.2 seconds apart. Note the temporal "spreading" of the temperature variations around the leading edge due to the movement of the necklace vortices toward the juncture.

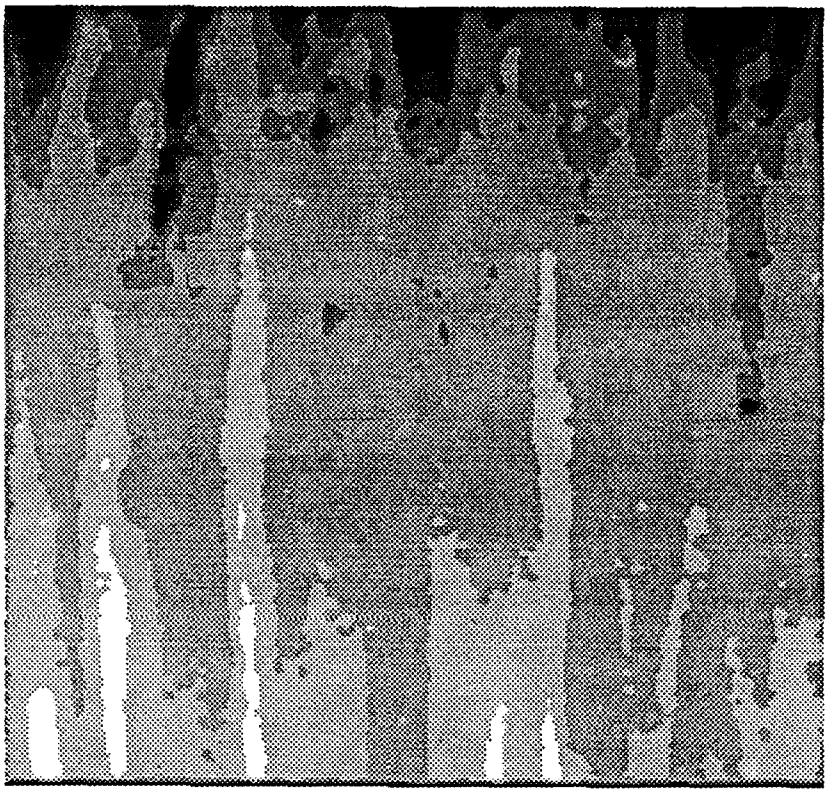

Figure 15. An example of the temperature field beneath a tripped, turbulent boundary layer at $Re_\theta = 800$; flow is top-to-bottom. Note the presence and spanwise distribution of temperature "streaks", comparable to the low-speed streaks in a turbulent boundary layer. Each gray-level represents a temperature variation of 1°C.